Journal of Molecular Graphics and Modelling 53 (2014) 92–99

Contents lists available at ScienceDirect

Journal of Molecular Graphics and Modelling

journal homepage: www.elsevier.com/locate/JMGM

Analysis of the structure and morphology of fenoxycarb crystals

Jacek Zeglinski[a,*], Michael Svärd[a,b], Jolanta Karpinska[c], Manuel Kuhs[a], Åke C. Rasmuson[a,b]

[a] Materials and Surface Science Institute, Chemical and Environmental Sciences Department, University of Limerick, Limerick, Ireland
[b] Department of Chemical Engineering and Technology, KTH Royal Institute of Technology, Stockholm, Sweden
[c] School of Chemistry, National University of Ireland, Galway, Ireland

ARTICLE INFO

Article history:
Accepted 12 July 2014
Available online 19 July 2014

Keywords:
Crystal morphology
Crystal growth
Single crystal X-ray diffraction
Surface structure
Molecular modelling

ABSTRACT

In this paper, we have explored the relationship between surface structure and crystal growth and morphology of fenoxycarb (FC). Experimental *vs.* predicted morphologies/face indices of fenoxycarb crystals are presented. Atomic-scale surface structures of the crystalline particles, derived from experimentally indexed single crystals, are also modelled. Single crystals of fenoxycarb exhibit a platelet-like morphology which closely matches predicted morphologies. The solvent choice does not significantly influence either morphology or crystal habit. The crystal morphology is dominated by the {0 0 1} faces, featuring weakly interacting aliphatic or aromatic groups at their surfaces. Two distinct modes of interaction of a FC molecule in the crystal can be observed, which appear to be principal factors governing the microscopic shape of the crystal: the relatively strong collateral and the much weaker perpendicular bonding. Both forcefield-based and quantum-chemical calculations predict that the aromatic and aliphatic terminated {0 0 1} faces have comparably high stability as a consequence of weak intermolecular bonding. Thus we predict that the most developed {0 0 1} surfaces of fenoxycarb crystals should be terminated randomly, favouring neither aliphatic nor aromatic termination.

1. Introduction

Crystal morphology depends on the relative orientation and growth rates of the crystal faces. The velocity of growth usually varies from face to face and, according to Wulff's thermodynamic theory of crystal growth, the equilibrium shape of a crystal is related to the free energies of the crystal faces, meaning that crystal faces grow at rates proportional to their respective surface energies [1]. A systematic insight into these fundamental relations is therefore essential in order to understand and control crystallization processes at both laboratory and industrial scale.

The thermodynamic stability of a non-defective crystal surface is dependent on its chemical nature, *i.e.* which functional groups are exposed at the surface and their affinity for intermolecular interactions. Hence, a thorough understanding of crystal growth and morphology is often impossible without a detailed description at the atomic level. Knowledge of the surface structure of a crystal would give essential information to help rationalize phenomena at the solid–liquid interface, such as the solvent influence on directing the growth of a crystal in solution. Together with the crystal structure, face indexing of a crystal can be employed to obtain atomic level description of the idealized (non-defective) crystal surfaces. The applicability of such an approach has been demonstrated recently in rationalization of solvent effects on crystal morphology of tolbutamide [2] and thiadiazoles [3].

Here we apply the above discussed structure–property approach in an effort to understand the origin of the crystal morphology of fenoxycarb (FC), a complex flexible organic molecule (Fig. 1). Fenoxycarb, or 2-(*p*-phenoxyphenoxy)ethylcarbamate, is an insect growth regulator with juvenile hormone activity [4]. Its melting temperature and enthalpy are reported as 53.2 °C and 28.0 kJ mol^{-1}, respectively [5]. We recently reported its crystal structure for the first time [6]. Our recent study on nucleation kinetics of fenoxycarb revealed that its crystal nucleation in isopropanol largely depends on the thermal pretreatment of the solution, thus exhibiting the so-called "history of solution" effect [7].

In this contribution we present for the first time the experimental morphology and face indexing of fenoxycarb single crystals. The FC morphology is also studied in a range of solvents. The idealized crystal surfaces are modelled to give an atomic-level description of the respective experimentally indexed faces. The vacuum morphology of FC crystals is predicted with the BFDH and attachment energy methods, and compared with experimental results. In addition, we propose a facile method of estimating intermolecular interactions

* Corresponding author. Tel.: +353 61 23 41 57.
E-mail address: jacek.zeglinski@ul.ie (J. Zeglinski).

http://dx.doi.org/10.1016/j.jmgm.2014.07.008
1093-3263/

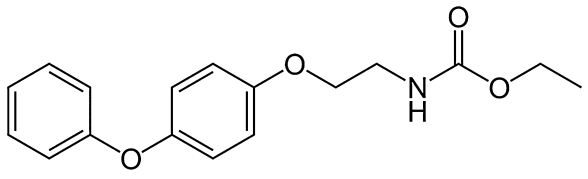

Fig. 1. Chemical structure of fenoxycarb.

in a crystal lattice at the quantum-chemical level by employing large crystalline cluster models.

We believe that this combined experimental and modelling study will aid better atomic-level understanding of crystal growth of a complex organic molecule. Furthermore, other macroscopic properties of the FC crystal, such as its low thermal stability, may now be rationalized at the atomic level.

2. Experimental

Fenoxycarb (>98.8%) from Syngenta, Switzerland was used directly without further purification. Fenoxycarb crystals were recrystallized by nucleation and growth from homogeneous solutions by slow evaporation of solvent. The effect of solvent on crystal shape and morphology was evaluated in ethanol, methanol, isopropanol, ethyl acetate, and toluene. About 1 mL of undersaturated solutions of fenoxycarb were prepared in glass vials at room temperature. The vials were sealed by parafilm and punctured with 2–3 small holes to allow for evaporation to dryness in about 5 days. By slow evaporation, the growth should proceed under low supersaturation, and the crystal shape should essentially be governed by thermodynamics.

An Oxford Diffraction Xcalibur system was used to collect X-ray diffraction data at 150 K. Face indexing was performed on single crystals of FC grown from ethanol with the Oxford program suite CrystAlisPro, version 171.34.36.

3. Computational methodology

The vacuum morphology was predicted using two methods: (i) the BFDH method [8], where face growth rates are assumed to be inversely proportional to the interplanar spacings in the lattice, and (ii) the attachment energy method, in which the growth rate of each crystal face is assumed to be proportional to the attachment energy, *viz.* the energy released upon attachment of a growth slice to a given crystal face. Calculations were done with Materials Studio 5.0 from Accelrys Inc., and the generic force field PCFF [9], parameterized for organic molecules, used together with built-in point charges; a combination that has been found to work adequately for similar systems in a previous study [10].

An electrostatic potential surface, which illustrates charge distribution of a molecule, was calculated for the fenoxycarb dimer being extracted from the crystal structure, using the MOLDEN software [11] with a grid density of 0.02. Fitting of electrostatic potential was based on the quantum-chemically derived multipole moments of the structure optimized at the B97D/6-31G(d,p) level with the GAUSSIAN 09 suite [12].

Density functional theory calculations were employed to quantify intermolecular interactions between the molecules of the FC crystal. The model structures were constructed as follows. A cluster consisting of a bunch of seven FC molecules was cut from a single molecular layer of a FC crystal supercell with a central (core) FC molecule surrounded by a cylindrical shell of six neighbouring FC molecules (structure **1**, Fig. 2). These clusters feature hydrogen bonds and π-interactions as in the monolayers forming the FC crystal. To quantify lateral interactions between the monolayers, *i.e.* the aliphatic-to-aliphatic and aromatic-to-aromatic binding at the (0 0 1) interface, two additional structures were constructed. Two pairs of fenoxycarb tetramers were cut from a FC crystal supercell with aliphatic-to-aliphatic (structure **2**) and aromatic-to-aromatic (structure **3**) orientations at the (0 0 1) interface. It is well known that the coordinates of light atoms such as hydrogens cannot be determined with sufficient precision from a single crystal XRD experiment. To improve the model structures while preserving their crystal geometry, we performed constrained optimization; only hydrogen atoms were allowed to relax while all other atoms were kept frozen during the optimization run. The geometries were calculated with a B97-D3 Grimme's functional [13], and a Gaussian-type 6-31G(d,p) basis set [14].

The binding of the core FC molecule to the shell FC molecules (structure **1**) was calculated as follows:

$$\Delta E_{\text{core–shell}} = E_{\text{cluster}} - (E_{\text{shell}} + E_{\text{core}}) \quad (1)$$

where E_{cluster} is a single point energy of a cluster combined of 7 FC molecules, E_{shell} a single point energy calculated for a shell structure made after removing the core FC molecule from the cluster, and E_{core} a single point energy calculated for that removed core FC molecule (see Fig. 2). A pair interaction of a core FC molecule with a selected molecule of a second shell was calculated as follows:

$$\Delta E_{\text{C–X}} = E_{\text{C–X}} - (E_{\text{C}} + E_{\text{X}}) \quad (2)$$

where $E_{\text{C–X}}$ is a single point energy of a C–X pair of molecules after removing the others FC molecules form the structure **1a**, and E_{C} and E_{X} are single point energies of the isolated molecules C and X.

The intermolecular interactions at the (0 0 1) interface (structures **2** and **3**, Fig. 3) were calculated as follows:

$$\Delta E_{\text{aliphatic interface}} = E_{\text{ali–ali}} - 2E_{\text{tetramer}} \quad (3)$$

$$\Delta E_{\text{aliphatic interface}} = E_{\text{arom–arom}} - 2E_{\text{tetramer}} \quad (4)$$

where $E_{\text{ali–ali}}$ and $E_{\text{arom–arom}}$ are energies of molecular clusters consisting of two FC tetramers with respective aliphatic-to-aliphatic and aromatic-to-aromatic orientations of end groups, and E_{tetramer} is the energy of an isolated FC tetramer.

In the unit cell of fenoxycarb there are two symmetry-unrelated molecules having different conformations (Fig. 4). We have performed control calculations by considering another core–shell cluster model with the core FC molecule being in the second conformation. We found that the difference in the core–shell binding energy between the two clusters is small (less than 3.5% of the $\Delta E_{\text{core–shell}}$); thus regardless of the conformation each FC molecule in the crystal lattice on average experiences comparable intermolecular interactions.

The interaction energies were calculated with a double-hybrid B2PLYPD3 functional [15] which combines exact Hartree–Fock exchange with MP2-like correlation and long-range dispersion corrections. A large basis set of def2-TZVPP quality [16] was used in all the energy calculations. Calculations were performed using the GAUSSIAN 09 package [12].

4. Results and discussion

4.1. Crystal structure and intermolecular interactions

The crystal structure of fenoxycarb [6] belongs to the triclinic crystal system with the centrosymmetric $P\bar{1}$ (C_i) space group. The unit cell is occupied by four fenoxycarb molecules and is elongated in the *c*-direction as shown in Fig. 4. The fenoxycarb molecules are 'frozen' in the crystal lattice in four distinct conformations, where A1 and A2, and B1 and B2, respectively, are mirror-images related by an inversion centre.

A FC molecule is composed of two parts separated by an ether bridge: the aromatic part combines two benzene rings, separated

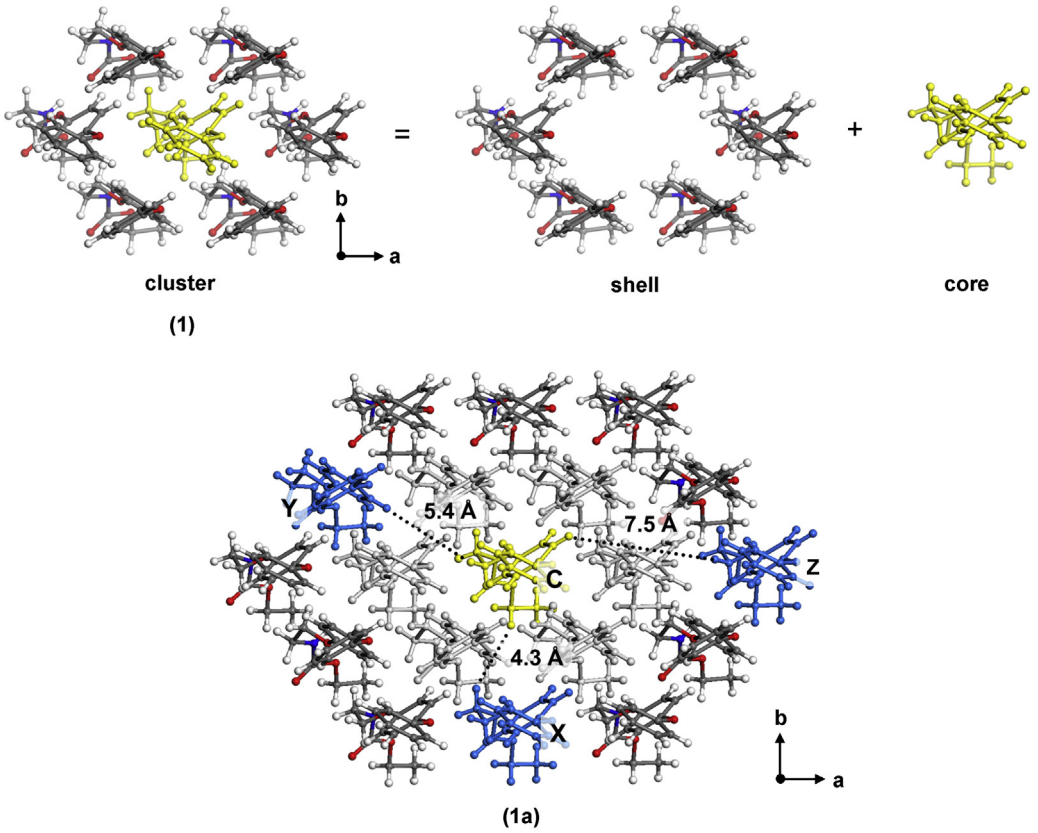

Fig. 2. (Top) A fenoxycarb cluster consisting of seven FC molecules cut from the crystal (structure **1**). The first shell and core components of the cluster are shown, with the core FC molecule highlighted in yellow. (Bottom) A cluster (**1a**) consisting of first and second shell of FC molecules. Molecules denoted as X, Y, and Z (in blue) are used for computing pair interactions with the central FC molecule (in yellow). (For interpretation of the references to colour in this figure legend, the reader is referred to the web version of this article.)

by another ether bridge, and the aliphatic part is made up of an ethylene (—CH_2—CH_2—), a carbamate (—NHCOO—), and an ethyl (—CH_2—CH_3) group.

Fig. 5a shows the electrostatic potential surface of two neighbouring FC molecules in the crystal lattice. For the purpose of computations the structure was optimized as an isolated dimer. Nevertheless, the geometry after gas-phase relaxation varies only slightly from that in the crystal lattice. The electrostatic potential surface gives qualitative information on electrostatic interactions between molecules. This feature can be used in rationalizing the molecular recognition mechanism. It can also be useful in qualifying weak interactions in molecular crystals – a property not always accessible with other methods.

The electrostatic potential map indicates electron-rich (red) and electron-deficient (blue) regions in the fenoxycarb dimer. The electron-rich negative domains surround all the oxygen atoms, being most pronounced at the carbonyl oxygen. Interestingly, the π-electron clouds are also clearly marked as yellow-red circles. The deep-blue colour on the amide hydrogen indicates a more positive potential and higher affinity for bonding to electron-rich species. On the other hand, the light-blue surface at the carbohydrate hydrogens indicates that weak binding interactions with electronegative atoms or π-electron clouds are plausible.

From the electrostatic potential map it appears that molecules of fenoxycarb are stabilized in the crystal lattice by a combination of (i) weak interactions, including C—H. . .O(ether) and π-aromatic ring–H-benzene interactions, and (ii) strong hydrogen bonding between amide hydrogen and carbonyl oxygen. The N—H. . .O=C hydrogen bonds separate adjacent FC molecules at 1.940 Å and 1.956 Å.

The aromatic parts of fenoxycarb molecules are located in the crystal lattice close to each other and form an array where each conformer type creates a layer of parallel-displaced benzene rings (Fig. 5b). The layer of type (A1) interacts with the layer of type (B1) conformers, creating a cyclic arrangement of three phenyl groups.

A theoretical study on π-interactions in benzene dimers and trimers has indicated that the cyclic arrangement of aromatic rings yields the strongest attractions compared to other possible configurations, such as sandwich, parallel-displaced, and T-shaped [17].

The strength of binding between aromatic rings in the fenoxycarb crystal can be approximated based on these *ab initio* calculations with the reported binding energy of 6.7 kJ mol^{-1} per two benzene molecules in a cyclic trimer. It is worth noting that every benzene ring in a single molecular layer of the FC crystal is surrounded by six other benzene rings and hence the cyclic arrangement of the rings facilitates their optimum binding and implies higher thermodynamic stability to the local structure.

In this work we have quantified the intermolecular interactions in the FC crystal by quantum-chemical calculations. The FC crystal structure is layered, with well-defined slip planes between the layers. Within such a layer, a single FC molecule interacts directly with six other FC molecules, and this feature can be captured in a simple cluster model consisting of seven FC molecules (structure **1**, Fig. 2). The remaining out-of-layer interactions, *viz.* those at the aromatic and aliphatic ends of the FC molecule, are shown in Fig. 3 (structures **2** and **3**).

Table 1 collates the DFT binding energies for structures **1**–**3**. Our calculations indicate that the bonding of one FC molecule to six adjacent FC molecules in the crystal ($\Delta E_{core-shell}$ = −158.16 kJ mol^{-1}, structure **1**) is significantly stronger than the

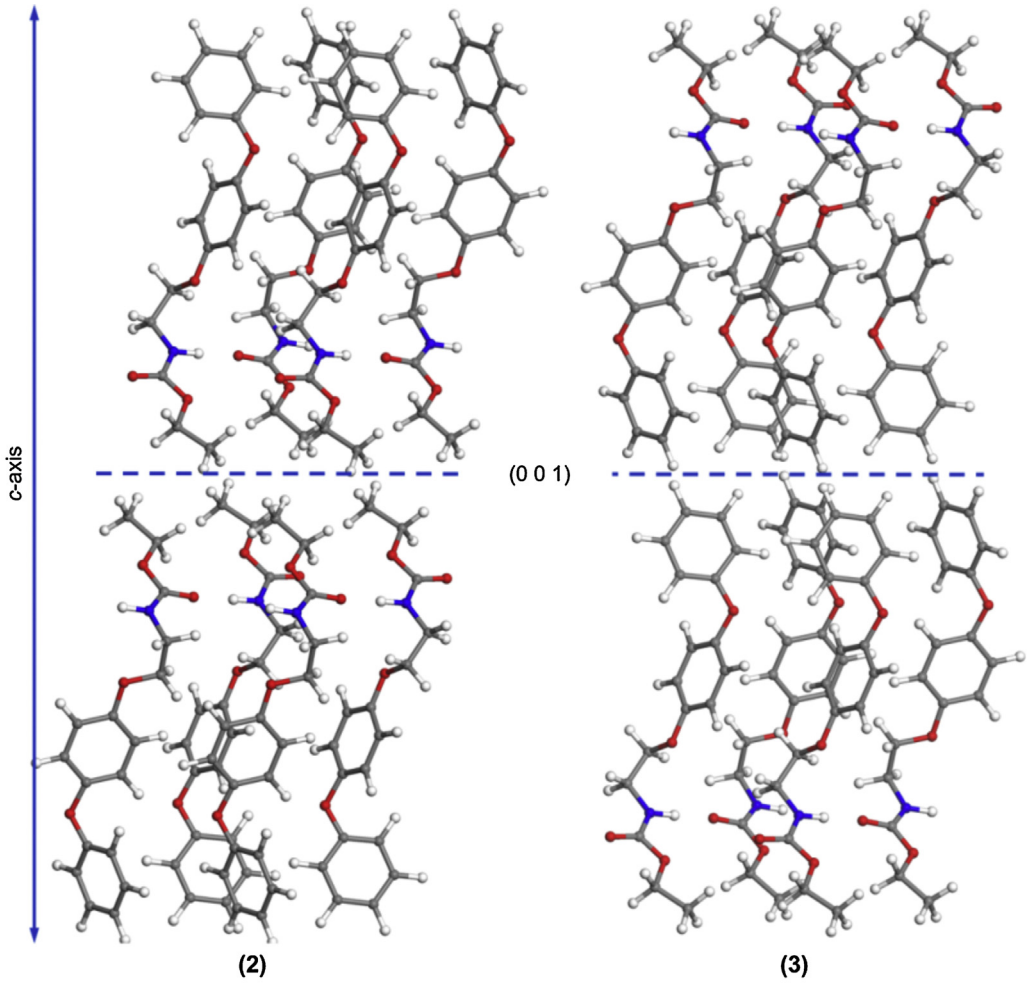

Fig. 3. Two pairs of FC tetramers at the (0 0 1) interface with (**2**) aliphatic-to-aliphatic, and (**3**) aromatic-to-aromatic molecular orientations as in the FC crystal. The structures preserve crystal geometry; only hydrogen atoms are optimized at DFT B97-D3/6-31G(d,p) level.

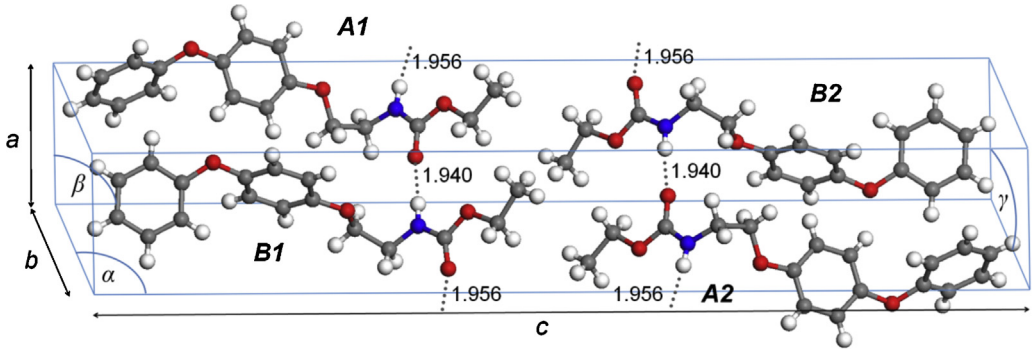

Fig. 4. Unit cell of fenoxycarb from single crystal XRD refinement [6]: $a = 5.903$ Å, $b = 7.571$ Å, $c = 35.373$ Å, $\alpha = 85.62°$, $\beta = 86.21°$, $\gamma = 89.05°$. A1, A2, B1 and B2 indicate different molecular conformations. H-bonds of N—H. . .O═C are shown as dotted lines with distances in Ångstroms; carbon – grey, hydrogen – white, oxygen – red, nitrogen – blue. (For interpretation of the references to colour in this figure legend, the reader is referred to the web version of this article.)

interaction of $-2.20\,kJ\,mol^{-1}$ at the aliphatic (structure **2**) and of $-2.22\,kJ\,mol^{-1}$ at the aromatic (structure **3**) interface of the (0 0 1) plane. The intermolecular binding energy, $\Delta E_{core-shell}$, does not include long-range van der Waals interactions which are present in an infinite crystal lattice. To estimate an effect of these non-specific interactions we computed the binding energy between a selected molecule of the second shell of the crystalline cluster and the core FC molecule (*cf.* structure **1a**, Fig. 2). Our computations show that the bonding of the second shell molecules ranges from $-3.23\,kJ\,mol^{-1}$ to $-0.30\,kJ\,mol^{-1}$ at a distance of 7.5–4.3 Å. If we consider that in the extended cluster **1a** there are two FC molecules at a distance of 4.3 Å (C–X), eight molecules at *ca.* 5.4 Å (C–Y), and another two molecules at 7.5 Å (C–Z), than an approximate binding of a whole second shell to the core FC molecule equals $-13.30\,kJ\,mol^{-1}$ as calculated as a sum of these pair interactions. These results show that the interactions with the second shell are more than one order of magnitude weaker compared to those of the first shell ($\Delta E_{core-shell}$) but they are not negligible. After

Table 1
Binding energies (kJ mol^{-1}) of a single fenoxycarb molecule in its crystal lattice: $\Delta E_{\text{core–shell}}$ (structure **1**), $\Delta E_{\text{aliphatic interface}}$ (structure **2**), and $\Delta E_{\text{aromatic interface}}$ (structure **3**). Pair interactions of the core FC molecule with the X, Y, and Z molecules of the second shell are denoted as $\Delta E_{\text{C–X}}$, $\Delta E_{\text{C–Y}}$, and $\Delta E_{\text{C–Z}}$, respectively. The binding energies are calculated at the DFT B2PLYPD3/def2-TZVPP level.

$\Delta E_{\text{core–shell}}$	$\Delta E_{\text{aliphatic interface}}$	$\Delta E_{\text{aromatic interface}}$	$\Delta E_{\text{C–X}}$	$\Delta E_{\text{C–Y}}$	$\Delta E_{\text{C–Z}}$
−158.16	−2.20	−2.22	−3.23	−0.78	−0.30

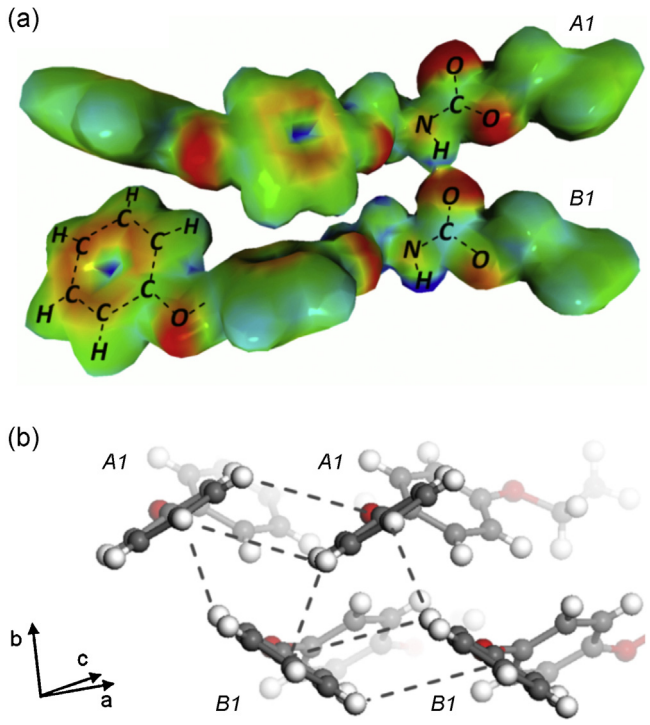

Fig. 5. Electrostatic potential surface of fenoxycarb dimer consisted of A1 and B1 conformers (a), blue – positive, red – negative, green – neutral potential. Molecular arrangement of aromatic rings in fenoxycarb crystal (b). Dashed lines indicate π-aromatic ring–H-benzene interactions.

including the second shell interactions, the bonding of FC molecule in a single layer of the crystal is about −171.5 kJ mol^{-1}.

4.2. Interrelationship of surface structure, crystal growth and morphology

Crystal growth by slow solvent evaporation yielded large, translucent crystals with a platelet habit, as well as small yellow granules with rough surfaces. We have found that the choice of solvent does not noticeably affect the habit or size distribution of the resultant crystals, and as explored in previous work [18], fenoxycarb apparently shows no propensity for polymorphism. Fig. 6 shows large crystals grown from ethanol, along with vacuum crystal morphologies of fenoxycarb computationally predicted with two methods. SEM images in Fig. 7 show some morphological features of the crystalline particles grown from four different solvents. Fig. 7(a), (b) and (d) shows non-uniform edges of the particles, while Fig. 7(c) highlights steps at the crystal surface.

In Table 2, calculated attachment energies and crystal facets (symmetrically identical sets of faces) predicted with the attachment energy method are given, together with the corresponding area fraction of each respective crystal facet.

As can be seen, the calculated plate-like habit closely matches the experimentally obtained crystal shapes. The force field calculations predict that the two {0 0 1} faces, *i.e.* (0 0 1) and

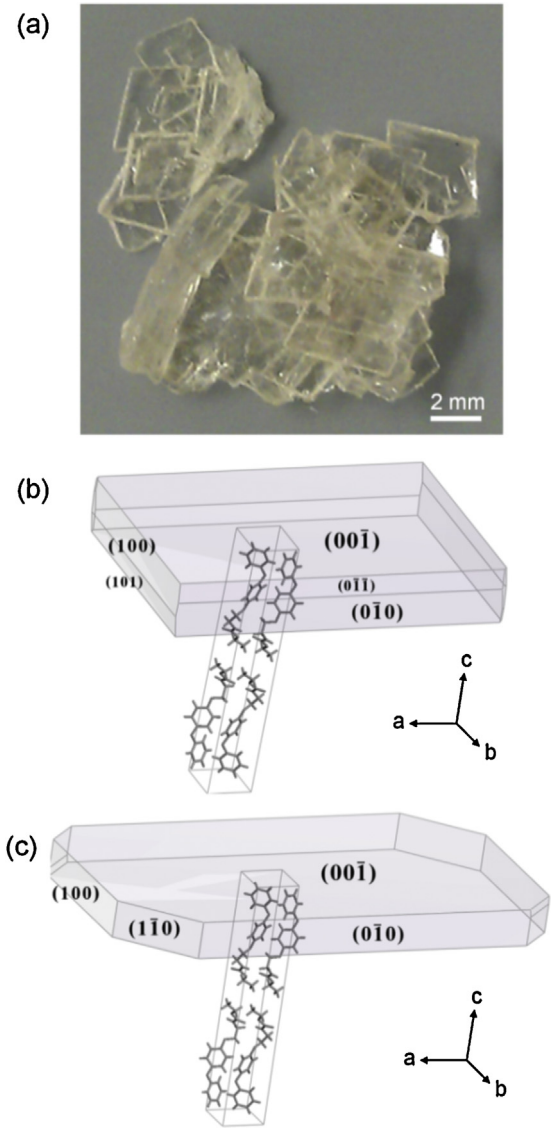

Fig. 6. Morphology of crystalline fenoxycarb: macroscopic crystals grown by slow evaporation of solvent (a), the vacuum morphology as predicted by the BFDH method (b), and the attachment energy method (c). Miller indices are given for major faces, together with unit cell representation.

Table 2
Calculated attachment energy and total area for stable configurations of facets predicted with the attachment energy method.

Facet {*h k l*}	E_{att} (kJ mol^{-1})	Area (%)
{0 0 1}	−9.5	83.5
{0 1 0}	−81.4	8.0
{1 0 0}	−107.9	4.9
{1 −1 0}	−109.7	2.4
{1 1 0}	−123.5	1.0

(0 0 −1), should dominate the morphology of fenoxycarb crystals, followed by the less pronounced {0 1 0} and {1 0 0} sets of faces. The two prediction methods differ only slightly with respect to other visible faces and their relative areas.

During experimental crystal growth from ethanol, it was observed that crystals initially form laths, and as they grow, become more plate-like. We attempted to index those single crystals at different stages of growth. However, only the lath-like crystals were of sufficient quality to allow for unambiguous indexation of the crystal faces (Fig. 8). As can be seen, the dominant faces of the single

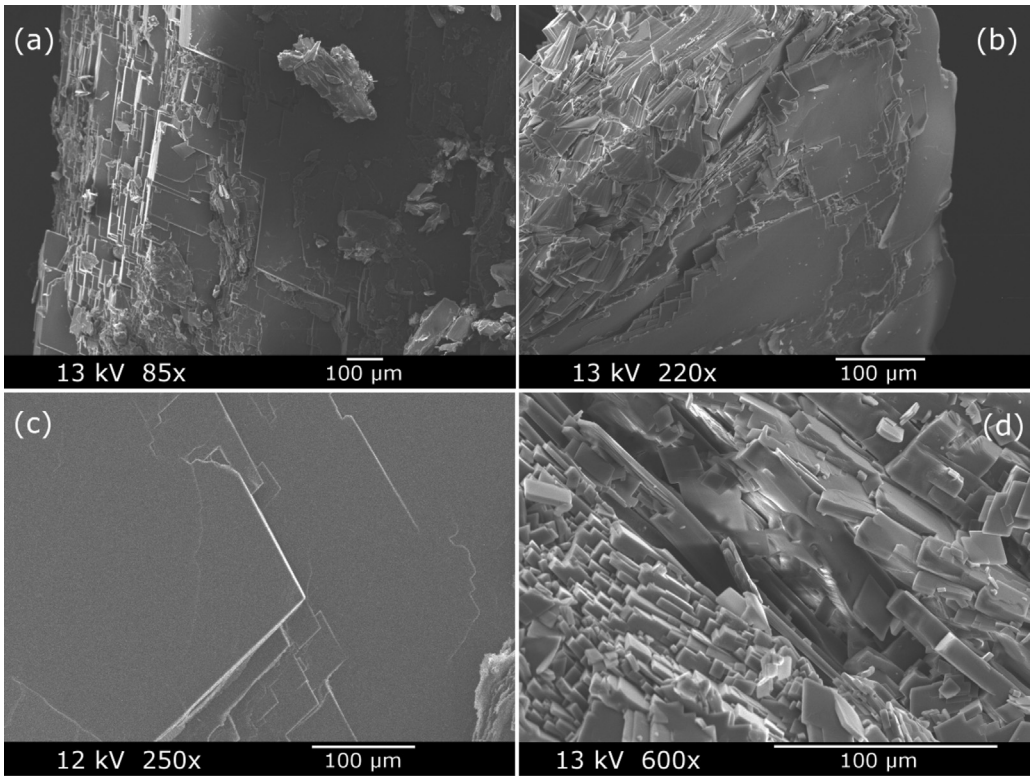

Fig. 7. SEM micrographs showing layered nature of crystalline fenoxycarb, grown from (a) ethyl acetate, (b) toluene, (c) ethanol, and (d) isopropanol (magnified view of the particle edge).

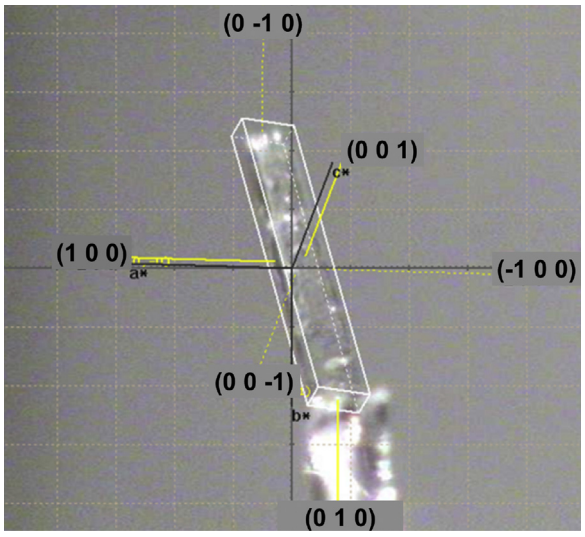

Fig. 8. Experimental face indexing of fenoxycarb crystals grown from ethanol.

crystal of FC are (0 0 1) and (0 0 −1), in agreement with the predicted morphology. The crystal also exhibits the (0 1 0), (0 −1 0) and the (1 0 0), (−1 0 0) pairs of faces – this also matches the predicted morphology. The {1 1 0} and {1 −1 0} faces, which are featured in the predicted morphology when employing the attachment energy method, albeit with very low surface area and the highest attachment energies, could not be experimentally detected in lath-shaped crystals.

The molecular arrangement of experimentally observed faces is shown in Fig. 9. The lowest attachment energy (smallest negative value) of −9.5 kJ mol^{-1} has been calculated for the major (most developed) {0 0 1} faces (Fig. 9a). The lowest energy value indicates the weakest interactions and hence the slowest growth-rate of the crystal in the direction normal to the plane. This, in turn, is clearly reflected in the predicted crystal morphology, where the {0 0 1} faces account for 83.5% of the total area of a simulated particle. Parallel to the plane of the {0 0 1} faces are the hydrogen bond chains so no H-bonding is possible at this surface. Also, the aromatic rings are stacked parallel to this crystal plane, resulting in π-interactions parallel to the face. The second and third most important groups of faces predicted, {0 1 0} (Fig. 9b) and {1 0 0} (Fig. 9c), are capable of binding molecules about 10 times stronger than the {0 0 1} faces, with calculated attachment energies of −81.4 kJ mol^{-1} and −107.9 kJ mol^{-1}, respectively. The high attachment energy values indicate strong interactions and fast growth and hence less developed faces. This matches the experimental plate-like rectangular shapes of the macroscopic crystals (Fig. 6a).

At a molecular level, the {0 1 0} and the {1 0 0} faces are extended parallel to the crystal plane, resulting in both polar groups and benzene rings being exposed at the surface, and thus accessible for potential H-bond and π-interactions. For the {1 −1 0} face, the amide and carbonyl groups form chains of H-bonds nearly parallel to this plane, thus H-bonding is hardly accessible on this surface (see Fig. 9, structure (d)). This is noticeably different from the {0 1 0}, {1 0 0}, and {1 1 0} faces, where the chains of H-bonds are at an angle of 45–90° relative to their respective crystal planes, and the free (non-H-bonded) polar amide and carbonyl groups are exposed on these surfaces.

Since there is a clear resemblance between predicted and experimental morphologies, the crystal shape appears to be primarily governed by the difference in the strength of interactions between fenoxycarb molecules at different directions in the crystal lattice. The main feature of all the surfaces experimentally determined to be fast-growing is that the fenoxycarb molecules lie horizontally in the plane of the crystal face, contrary to the slow-growing {0 0 1} faces, where the molecules are oriented perpendicular to the crystal

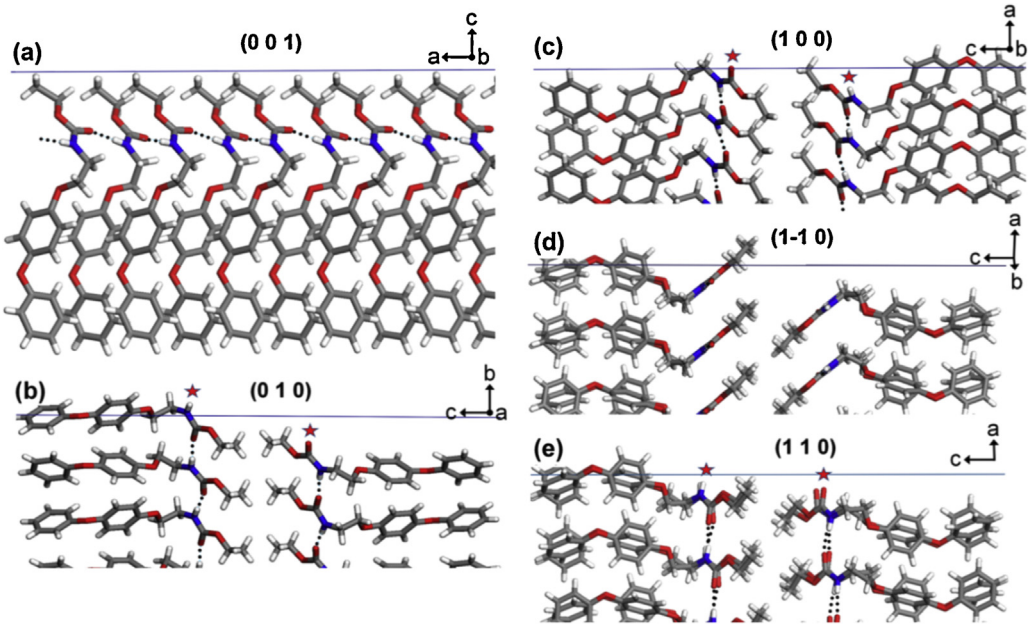

Fig. 9. Molecular representations of experimentally observed faces of fenoxycarb crystals. The slowest-growing (0 0 1) face (a), and faster growing faces (b–e): (0 1 0) (b), (1 0 0) (c), (1 −1 0) (d), and (1 1 0) (e). Hydrogen bonds of N—H. . .O═C in neighbouring fenoxycarb molecules are shown as dotted lines, and surface non-H-bonded N—H and C═O groups are marked with red stars. (For interpretation of the references to colour in this figure legend, the reader is referred to the web version of this article.)

plane. The growth direction is primarily governed by a combined intermolecular attraction through unsaturated amide and carbonyl H-bond donors and acceptors, along with π-interactions of benzene rings and other weakly interacting groups such as C—H. . .O(ether). However, the crystal growth is of course not entirely governed by H-bond interactions, as shown by the predicted fast growing {1 −1 0} faces which do not exhibit easily accessible hydrogen bonding groups (Fig. 9d). In the case of these faces, crystal growth appears to be predominantly driven by interactions of benzene rings and van der Waals' forces of aliphatic backbones. The order of attachment energies between different faces given in Table 2 is not merely governed by the presence or absence of exposed hydrogen bonding polar groups at the respective surfaces. Interestingly, the {1 −1 0} faces, though not possessing distinct H-bonding capabilities, exhibit the second highest attachment energy of −109.7 kJ mol^{-1} and thus are expected to grow faster than the H-bond donating and accepting {0 1 0} and {1 0 0} faces, with their respective attachment energies of −81.4 kJ mol^{-1} and −107.9 kJ mol^{-1}. This points to the fact that, especially in the case of large, oriented molecules, hydrogen bonding at the surface may not always be the dominant contributor to the total binding/attachment energy.

The slowest-growing faces, and thus the most developed, are the {0 0 1} faces, which can be terminated either with aromatic or aliphatic groups. The forcefield-calculated attachment energies for the aromatic-terminated and aliphatic-terminated faces are −10.6 kJ mol^{-1} and −9.5 kJ mol^{-1}, respectively; values that are higher than the binding energies estimated by DFT of −2.20 kJ mol^{-1} and −2.22 kJ mol^{-1} (Table 1). In spite of the differences in absolute numbers, both computational methods consistently predict the aromatic and aliphatic terminated {0 0 1} faces to have similar, high stability. Thus we predict that the most developed {0 0 1} faces of real fenoxycarb crystals should be terminated randomly, favouring neither aliphatic nor aromatic termination. The two distinct modes of interaction present in the fenoxycarb crystal lattice, *i.e.* the relatively strong collateral and the much weaker perpendicular intermolecular binding, may influence not only the crystal growth mechanism but also other physical properties of the crystal, such as its mechanical and thermal

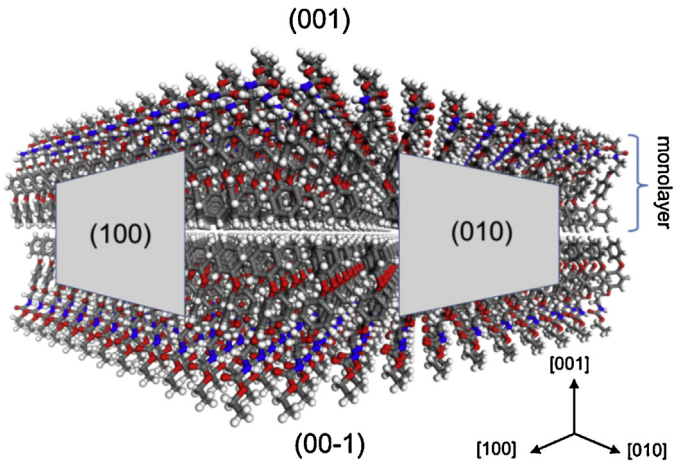

Fig. 10. A model crystal particle consisting of 480 molecules of FC (7 nm × 7 nm × 3.4 nm) with aromatic-to-aromatic end-groups located at the interface between monolayers and aliphatic end-groups at the top (0 0 1) and bottom (0 0 −1) surface.

properties. It could be argued that the FC crystal should be more durable when applying a force normal to the (0 0 1) plane, *i.e.* in a [0 0 1] direction, whereas it should be much easier to cleave a particle when applying force in a direction parallel to the monolayers (see Fig. 10).

Regarding thermal properties, the weak intermolecular binding between the monolayers at the {0 0 1} interface could contribute to the low thermal stability of the compound. The reported melting point of 53.16 °C [6] is relatively low compared to crystals made of molecules with similar molecular weight, *e.g.* fenofibrate which has a higher melting point of 80 °C despite having no hydrogen bonding present in the crystal lattice [19]. However, the fenofibrate structure exhibits a relatively isotropic, uniform distribution of intermolecular interactions, whereas the FC molecules are strongly bound within a monolayer but weakly bound at the interface between the monolayers.

5. Conclusions

Fenoxycarb crystals exhibit a platelet-like habit, which closely matches gas-phase morphologies computed with the BFDH and attachment energy methods. The choice of solvent does not significantly influence the crystal shape of slowly grown crystals. By single crystal face indexing, it is shown that the dominant and hence the slowest growing faces present in the fenoxycarb crystals are the {0 0 1} faces. The other indexed faces, accounting for a smaller fraction of a total surface area, are the {0 1 0} and {1 0 0} faces. The attachment energy method correctly predicts the existence of all these faces. With molecular modelling it is shown that the faces experimentally determined to be fast-growing feature fenoxycarb molecules oriented horizontally in the plane of the crystal faces, facilitating strong collateral intermolecular binding at those surfaces through H-bond-accessible polar N—H and C=O groups, as well as C—H. . .O(ether) and π-interactions of aromatic rings. The binding strength per molecule within a monolayer is estimated by DFT to be $-172\ kJ\ mol^{-1}$, while interactions through the {0 0 1} interface, between aliphatic or aromatic end-groups of the molecules, are calculated to be orders of magnitude weaker.

Acknowledgments

We acknowledge support from the Science Foundation Ireland (SFI), grant number 10/IN.1/B3038. J. Zeglinski acknowledges the SFI and Higher Education Authority funded Irish Centre for High-End Computing (ICHEC) for access to computational facilities. M. Svärd gratefully acknowledges funding from the Swedish Research Council (621-2010-5391). Finally, we acknowledge the donation of fenoxycarb material by Syngenta, Switzerland.

References

[1] G. Wulff, Z. Krystallogr, Mineral 34 (1901) 449–530.
[2] G.L. Destri, A. Marrazzo, A. Rescifina, F. Punzo, J. Pharm. Sci. 102 (2013) 73–83.
[3] F. Punzo, J. Struct. Mol. 1032 (2013) 147–154.
[4] P. Masner, M. Angst, S. Dorn, Pestic. Sci. 18 (1987) 89–94.
[5] S. Xiao-Hong, L. Yuan-Fa, T. Zhi-Cheng, J. Ying-Qi, Y. Jian-Wu, W. Mei-Han, Chin. J. Chem. 23 (2005) 501–505.
[6] J. Karpinska, M. Kuhs, A. Rasmuson, A. Erxleben, P. McArdle, Acta Crystallogr. E 68 (2012) 2834–2835.
[7] M. Kuhs, J. Zeglinski, Å.C. Rasmuson, Cryst. Growth Des. 14 (2014) 905–915.
[8] R. Docherty, G. Clydesdale, K.J. Roberts, P. Bennema, J. Phys. D: Appl. Phys. 24 (1991) 89–99.
[9] H. Sun, J. Phys. Chem. B 102 (1998) 7338–7364.
[10] M. Svärd, Å.C. Rasmuson, Ind. Eng. Chem. Res. 48 (2009) 2899–2912.
[11] G. Schaftenaar, J.H. Noordik, J. Comput. Aided Mol. Des. 14 (2000) 123–134.
[12] M.J. Frisch, G.W. Trucks, H.B. Schlegel, G.E. Scuseria, M.A. Robb, J.R. Cheeseman, et al., Gaussian 09, Revision D.01, Gaussian Inc., Wallingford, CT, 2013.
[13] S. Grimme, S. Ehrlich, L. Goerigk, J. Comput. Chem. 32 (2011) 1456–1465.
[14] V.A. Rassolov, M.A. Ratner, J.A. Pople, P.C. Redfern, L.A. Curtiss, J. Comput. Chem. 22 (2001) 976–984.
[15] L. Goerigk, S. Grimme, J. Chem. Theory Comput. 7 (2011) 291–309.
[16] F. Weigend, M. Häser, H. Patzelt, R. Ahlrichs, Chem. Phys. Lett. 294 (1998) 143–152.
[17] M.O. Sinnokrot, C.D. Sherrill, J. Phys. Chem. A 110 (2006) 10656–10668.
[18] M. Kuhs, M. Svärd, Å.C. Rasmuson, J. Chem. Thermodyn. 66 (2013) 50–58.
[19] A. Heinz, K.C. Gordon, C.M. McGoverin, T. Rades, C.J. Strachan, Eur. J. Pharm. Biopharm. 71 (2009) 100–108.